J|A|C|S ARTICLES

Published on Web 02/11/2009

Hydrazine-Linked Convergent Self-Assembly of Sophisticated Concave Polyhedrons of β-Ni(OH)$_2$ and NiO from Nanoplate Building Blocks

Wei Zhou,[†] Meng Yao,[†] Lin Guo,*[,†] Yueming Li,[‡] Jinghong Li,*[,‡] and Shihe Yang*[,†,§]

School of Chemistry and Environment, Beijing University of Aeronautics and Astronautics, Beijing 100191, China, Department of Chemistry, Tsinghua University, Beijing 100084, China, and Department of Chemistry, The Hong Kong University of Science and Technology, Clear Water Bay, Kowloon, Hong Kong, China

Received November 9, 2008; E-mail: guolin@buaa.edu.cn; jhli@mail.tsinghua.edu.cn; chsyang@ust.hk

Abstract: Intelligent self-assembly of nanobuilding blocks during the formation of Ni(OH)$_2$ single crystals with concave polyhedron structure was studied. The nickel hydroxide nanoplates pile up together with the aid of hydrazine molecules and grow along the [001] direction to form the brand-new geometry of concave polyhedrons. The novel nanostructure looks like a regularly twisted triangular prism wringed smoothly in the middle and could be attributed to the inherent spatial asymmetry of the nickel hydroxide crystal structure and the hydrogen bonds linked with the added hydrazine molecules. On the basis of the putative mechanism, polyhedrons with different longitudinal sizes (0.3−1 μm) were synthesized by adjusting the quantities of hydrazine. We also obtained NiO polyhedron crystals with similarly piled plates by calcinations of the Ni(OH)$_2$ polyhedrons. Our preliminary electrochemical experiments show that the Ni(OH)$_2$ polyhedrons have potential applications in electrochemical storage.

Introduction

The clever organization of nanobuilding blocks has been attracting increasing attention and enriching "bottom-up" approaches toward future nanodevices. Simple one-dimensional (1D) nanostructures can be obtained by the assembly of nanospheres.[1−3] Recently, researchers started to fabricate hierarchical nanomaterials with complex geometry by patterning nanobuilding blocks, including metals, oxides, sulfides, hydroxides, and other materials.[4−13] Various methodologies have been developed to achieve complicated architectures, such as thermal vapor deposition,[4,5] electrochemical deposition,[6,7] hydrothermal/solvothermal method,[8−10] microemulsion,[11] soft templating,[12,13] and microwave assistance.[14] Interestingly, many complex hierarchical nanostructures could be easily obtained by wet chemical routes. For example, Zhang et al. synthesized Cu_2O double tower-tip-like structures with microemulsion in a sealed Teflon-lined autoclave at 60 °C. It was believed that the cetyltrimethylammonium bromide (CTAB) adsorption on the primary rod guided the formation of the first few layers and initiating the heterogeneous nucleation process.[11] Pouget et al. reported highly ordered centimeter-long fibers obtained through self-organization assisted by double-walled silica nanotubes. They proposed a coupling mechanism whereby the spatiotemporal coordination regulates the templated-assembly, leading to macroscopic constructions with nanometric precision.[12] Inspired by these successes and learning from nature, we recognize that, for the fabrication of hierarchical architectures by mild chemical solution methods, the template action or the coupling force of small molecules is of fundamental importance for complex structures. Therefore, a simple synthesis to fabricate hierarchical concave polyhedron crystals, using N_2H_4-coupled self-assembly of β-Ni(OH)$_2$ nanoplates with a remarkable atomic precision was proposed.

Nickel hydroxide is an active material of the positive electrode of alkaline rechargeable batteries for its high power density, high energy, and low toxicity.[15] The performances of such batteries are directly affected by size and morphology, and the electrochemical performance can be improved by nanoscale

[†] Beijing University of Aeronautics and Astronautics.
[‡] Tsinghua University.
[§] The Hong Kong University of Science and Technology.

(1) Tang, Z.; Kotov, N. A.; Giersig, M. *Science* **2002**, *297*, 237–240.
(2) Pacholski, C.; Kornowski, A.; Weller, H. *Angew. Chem., Int. Ed.* **2002**, *41*, 1188–1191.
(3) Jun, Y.; Casula, M. F.; Sim, J.-H.; Kim, S. Y.; Cheon, J.; Alivisatos, A. P. *J. Am. Chem. Soc.* **2003**, *125*, 15981–15985.
(4) Sun, S.; Meng, G.; Zhang, G.; Masse, J.-P.; Zhang, L. *Chem.−Eur. J.* **2007**, *13*, 9087–9092.
(5) Hu, J.; Bando, Y.; Zhan, J.; Yuan, X.; Sekiguchi, T.; Golberg, D. *Adv. Mater.* **2005**, *17*, 971–975.
(6) Li, Y.; Li, C.; Cho, S. O.; Duan, G.; Cai, W. *Langmuir* **2007**, *23*, 9802–9807.
(7) Ren, G.; Zheng, F.-L.; Tong, Y.-X. *Cryst. Growth Des.* **2008**, *8*, 1226–1232.
(8) Ye, L.; Wu, C.; Guo, W.; Xie, Y. *Chem. Commun.* **2006**, 4738–4740.
(9) Wang, Q.; Xu, G.; Han, G. *Cryst. Growth Des.* **2006**, *6*, 1776–1780.
(10) Yang, L.-X.; Zhu, Y.-J.; Tong, H.; Liang, Z.-H.; Wang, W.-W. *Cryst. Growth Des.* **2007**, *7*, 2716–2719.
(11) Zhang, H.; Zhang, X.; Li, H.; Qu, Z.; Fan, S.; Ji, M. *Cryst. Growth Des.* **2007**, *7*, 820–824.
(12) Pouget, E.; Dujardin, E.; Cavalier, A.; Moreac, A.; Valéry, C.; Marchi-Artzner, V.; Weiss, T.; Renault, A.; Paternostre, M.; Artzner, F. *Nat. Mater.* **2007**, *6*, 434–439.
(13) Xu, H.; Wang, W. *Angew. Chem., Int. Ed.* **2007**, *46*, 1489–1492.
(14) Cao, H.; Gong, Q.; Qian, X.; Wang, H.; Zai, J.; Zhu, Z. *Cryst. Growth Des.* **2007**, *7*, 425–429.
(15) Chen, J.; Bradhurst, D. H.; Dou, S. X.; Liu, H. K. *J. Electrochem. Soc.* **1999**, *146*, 3606–3612.

nickel hydroxide.[16,17] So far, nickel hydroxide with various morphologies has been synthesized including nanoplates,[18] hollow spheres,[19] ribbonlike and boardlike structures,[20] flower-like structures,[10,21] and tubes.[17] However, three-dimensional organizations of higher-level structures of nickel hydroxide so far have not been reported.

Our work presented here creates a brand-new hierarchical structure in a bottom-up fashion. Benefiting from the inherent spatial asymmetry of $Ni(OH)_2$ and the hydrogen bonds linked with hydrazine molecules, hierarchical concave polyhedron achieves its intelligent growth with the 60° rotation between two parts of quasi-triangular-pyramids. This simple method for building up structures from nanoscale building blocks with the assistance of molecular linkage may be utilized for fabricating a wide variety of nanoarchitectures.

Experimental Section

All chemicals were of analytical grade and used without further purification. In a typical experiment, 0.128 g of nickel(II) 2,4-pentanedionate ($NiC_{10}H_{14}O_4$, 95%, Alfa Aesar) and 0.666 g of polyvinyl pyrrolidone (PVP, average MW 58000, K29−32, Acros) were first dissolved in 100 mL of deionized water at room temperature. Then the solution was heated to 75 °C in an oil bath under magnetic stirring. Afterward, 3 mL of hydrazine monohydrate liquid ($N_2H_4 \cdot H_2O$, 80%) was added into the mixture dropwise. In 30 min, 1.2 mmol sodium hydroxide solution (in 10 mL deionized water) was added. The reaction was maintained for 2 h at 75 °C (the precursor was obtained), and then 5 mL of $N_2H_4 \cdot H_2O$ was introduced. Then the solution was kept still for another 2 h. Afterward, the green precipitate was obtained and rinsed with ethanol and deionized water several times.

The as-prepared nickel hydroxide was transformed to nickel oxide by thermal decomposition in nitrogen at 500 °C for 1 h.

The structures and compositions of the as-prepared products were characterized by X-ray powder diffraction (XRD) using a Rigaku Dmax2200 X-ray diffractometer with Cu Kα radiation ($\lambda = 1.5416$ Å). The XRD specimens were prepared by means of flattening the powder on the small slides. The morphologies of the synthesized samples were studied by a field-emission gun (FEG) scanning electron microscope (Hitachi S-4800, 5 kV) with the samples obtained from the thick suspension dropping on the silicon slice. Transmission electron microscopy (TEM) and high-resolution TEM (HRTEM) investigations were carried out by a JEOL JEM-2100F microscope. The as-grown samples were dispersed in ethanol and dropped onto a carbon film supported on a copper grid for the drying process in air. Fourier transform infrared (FTIR) spectrum was recorded for a KBr diluted sample using a Nicolet Avatar 360 FT-IR spectrometer.

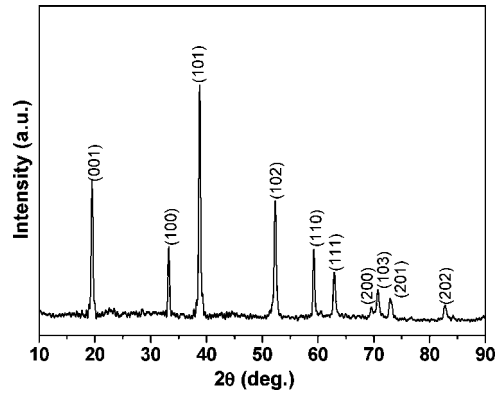

Figure 1. XRD pattern of the as-prepared sample.

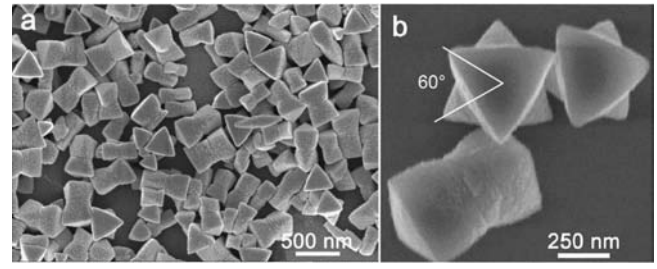

Figure 2. SEM images of the as-grown β-$Ni(OH)_2$. (a) Overhead view and (b) top and side views of typical polyhedrons. Each polyhedron is composed of two staggered truncated triangular pyramids.

The nickel electrodes were prepared as follows. The nickel hydroxide powder was mixed with black carbon and carboxymethyl cellulose as a binder in a weight ratio of 85:10:5. And then the mixture was incorporated into a nickel foam (1.2 × 1.2 cm) with spatula. The pasted nickel electrodes were dried at 80 °C and then pressed at a pressure of 5 MPa for 1 min. The cyclic voltammetry (CV) measurements were carried out on a Versa STAT 3 electrochemical workstation (Princeton Applied Research, USA). The cyclic voltammetry scan rate was 1 mV/s within a potential range from 0.1 to 0.64 V (vs Hg/HgO) at room temperature. The experiments were carried out in a three-electrode glass cell in which contained the nickel electrode as the working electrode, Pt foil as the counter electrode, Hg/HgO as the reference electrode, and 6 M KOH aqueous solution as the electrolyte.

Results and Discussion

Figure 1 presents the powder XRD pattern of the as-prepared products. All the diffraction peaks can be indexed as β-phase hexagonal nickel hydroxide (JCPDS 14-0117). No peaks due to α-$Ni(OH)_2$ were observed in the XRD pattern, which confirms the purity of the samples.

Typical SEM images of the nickel hydroxide are shown in Figure 2. Figure 2a is an overview of the samples with the concave polyhedron morphology. A peculiar morphology of elongated concave polyhedrons is evident with a length from 300 to 500 nm and with side lengths of the top triangles from 300 to 500 nm. A magnified image shown in Figure 2b provides top and side views of the structures. Obviously, the β-$Ni(OH)_2$ concave polyhedrons are composed of two staggered triangular pyramids truncated on the joined planes and rotated by an angle of 60° from each other. Each polyhedron has two regular triangles at the ends and six quasi-triangles at the sides. To join the two truncated pyramids together, the side quasi-triangles tend to develop curved surfaces instead of flat surfaces. Hence the novel nanostructure looks like a regularly twisted triangular prism wringed smoothly in the middle.

(16) (a) Che, G.; Lakshmi, B. B.; Fisher, E. R.; Martin, C. R. *Nature* **1998**, *393*, 346–349. (b) Han, X.; Xie, X.; Xu, C.; Zhou, D.; Ma, Y. *Opt. Mater.* **2003**, *23*, 465–470.
(17) Cai, F.-S.; Zhang, G.-Y.; Chen, J.; Gou, X.-L.; Liu, H.-K.; Dou, S.-X. *Angew. Chem., Int. Ed.* **2004**, *43*, 4212–4216.
(18) (a) Liang, Z.-H.; Zhu, Y.-J.; Hu, X.-L. *J. Phys. Chem. B* **2004**, *108*, 3488–3491. (b) Kong, X.; Liu, X.; He, Y.; Zhang, D.; Wang, X.; Li, Y. *Mater. Chem. Phys.* **2007**, *106*, 375–378. (c) Li, Y.; Tan, B.; Wu, Y. *Chem. Mater.* **2008**, *20*, 567–576. (d) Zhu, J.; Gui, Z.; Ding, Y.; Wang, Z.; Hu, Y.; Zou, M. *J. Phys. Chem. C* **2007**, *111*, 5622–5627.
(19) (a) Wang, D.; Song, C.; Hu, Z.; Fu, X. *J. Phys. Chem. B* **2005**, *109*, 1125–1129. (b) Duan, G.; Cai, W.; Luo, Y.; Sun, F. *Adv. Funct. Mater.* **2007**, *17*, 644–650.
(20) (a) Yang, D.; Wang, R.; Zhang, J.; Liu, Z. *J. Phys. Chem. B* **2004**, *108*, 7531–7533. (b) Yang, D.; Wang, R.; He, M.; Zhang, J.; Liu, Z. *J. Phys. Chem. B* **2005**, *109*, 7654–7658.
(21) (a) Cao, M.; He, X.; Chen, J.; Hu, C. *Cryst. Growth Des.* **2007**, *7*, 170–174. (b) Ni, X.; Zhang, Y.; Tian, D.; Zheng, H.; Wang, X. *J. Cryst. Growth* **2007**, *306*, 418–421. (c) Luo, Y.; Li, G.; Duan, G.; Zhang, L. *Nanotechnology* **2006**, *17*, 4278–4283.

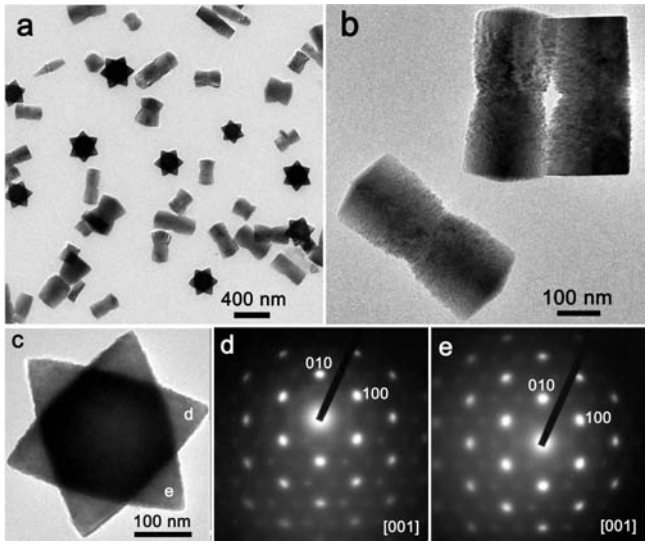

Figure 3. TEM images and SAED patterns of the as-grown β-Ni(OH)$_2$. (a) Overhead view, (b) side view of typical polyhedrons, (c) top view of the polyhedron, (d and e) SAED patterns corresponding to the two angles from the top and the bottom of the polyhedron marked in Figure 3c.

The nanostructures of as-prepared samples were further characterized by TEM. Figure 3 shows the TEM images and the selected area electron diffraction (SAED) patterns of the samples. An overview of the samples in Figure 3a is in good accordance with the SEM image in Figure 2a. The TEM images taken from the side and the top of the samples are shown in parts b and c of Figure 3, respectively, which further verify the concave polyhedron morphology. Figure 3b clearly reveals that the polyhedrons have rough edges and could be packed up layer by layer. Figure 3c exhibits that the polyhedron possesses regular triangles with each side length of ~300 nm. The SAED patterns of the area marked with d and e are shown in Figure 3. It can be seen that the two parts of one polyhedron possess single crystal structures. Both parts d and e of Figure 3 show the same set of diffraction spots of single crystal structure with the electron beam along the [001] direction, i.e., the *c* axis of β-Ni(OH)$_2$. It exhibits that the polyhedron is growing along the fixed [001] direction of crystal axis of nickel hydroxide.

To understand the formation of the polyhedron, the precursor was also characterized by XRD, TEM, and SEM, which was obtained by skipping the second step of adding hydrazine (see preparation in Experimental Section). It is gratifying to see that some hexagonal and quasi-hexagonal nanoplates with various sizes (the images of the SAED and XRD patterns are shown in Figure S1 of Supporting Information) were formed in the initial stage for the formation of polyhedrons. As shown in the SAED pattern in Figure S1 of Supporting Information, the axis of the nanoplate grows along [001] direction, according with the axis direction of the polyhedron (parts d and e of Figure 3), which further verifies that the quasi-hexagonal nanoplates are piled along the axis of [001], leading to the formation of the polyhedrons.

Next, seeing that hydrazine might play an important role for the formation of the hierarchical structure by adsorbing on the precursor plates and linking the plates together, control experiments were performed with less or more hydrazine added to the reacting system (see preparation of samples A and B in Supporting Information). When less hydrazine was added, the shorter polyhedrons with 300 nm in length and side length were obtained (sample A, Figure S2 of Supporting Information).

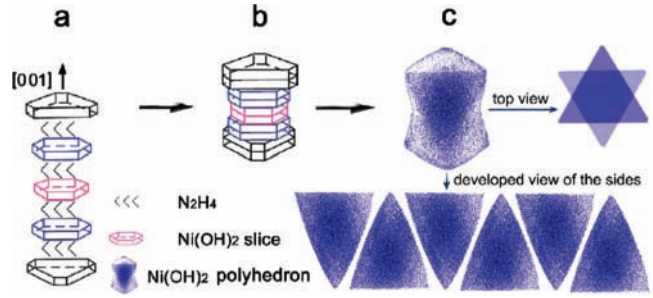

Figure 4. Schematic illustration for the formation of the concave polyhedron.

When more hydrazine was added, the concave polyhedrons became much longer (sample B, Figure S2 of Supporting Information). It was not unexpected that the average length of the polyhedrons could be controlled by changing the quantity of hydrazine. These results from above experiments confirm the cross-linking role of hydrazine on the formation of the polyhedrons.

To further prove the role of hydrazine in the formation process of the polyhedrons, we did another control experiment using $NH_3 \cdot H_2O$ instead of $N_2H_4 \cdot H_2O$, but only flowerlike structures composed of randomly stuck nanoplates were obtained (Figure S3 of Supporting Information). The schematic illustration in Figure S4 of Supporting Information shows how the two molecules of NH_3 and N_2H_4 affect the final morphology of the samples. The N_2H_4 molecule has two N atoms, so the molecule could link two layers of nickel hydroxide, and more and more layers can be assembled in this way. However, the NH_3 molecule has only one N atom; so with NH_3, the nickel hydroxide layers accumulate at random, forming the flowerlike structure. This experimental result strongly supports the existence of H bonds (N−H···O) for linking the nanoplates. Meanwhile, we recorded the FTIR spectrum of the polyhedron sample (Figure S5 of Supporting Information), and the FTIR result reveals that the N_2H_4 molecules link the Ni(OH)$_2$ plates by hydrogen bonds.

Additionally, some other control experiments were also carried out to check the role that the polymer PVP had played on the formation of the polyhedron. The experiment was carried out without PVP. However, the similar morphology (with the 60° rotation between the two quasi-triangular-pyramids) was obtained. The sample was not well grown with nonuniform sizes (Figure S6). This illustrates that the role of PVP could be eliminated for the growth mechanism of polyhedron. It was just to modify the polyhedron and lead to the well faceted structure and narrow size distribution.

On the basis of our experimental results, a probable formation mechanism of the Ni(OH)$_2$ polyhedron is proposed. When $N_2H_4 \cdot H_2O$ was added at the first time, the precursor nanoplates with different sizes were formed with the addition of sodium hydroxide. Then, they assembled by the linking force of N_2H_4 molecules which were selectively absorbed on the (001) planes of the hexagonal nickel hydroxide (as shown in Figure 4a). The piled sheets (in Figure 4b) were gradually growing together. As the (001) planes of Ni(OH)$_2$ were more stable, edges and corners of the nanoplates (in the middle part of the quasi-polyhedron) progressively disappeared to the benefit of more stable surfaces, i.e., (001) planes at the ends, via a process known as Ostwald ripening.[22] Then the rough surfaces of the

(22) (a) Roosen, A. R.; Carter, W. C. *Physica A* **1998**, *261*, 232–247. (b) Matijevic, E. *Chem. Mater.* **1993**, *5*, 412–426.

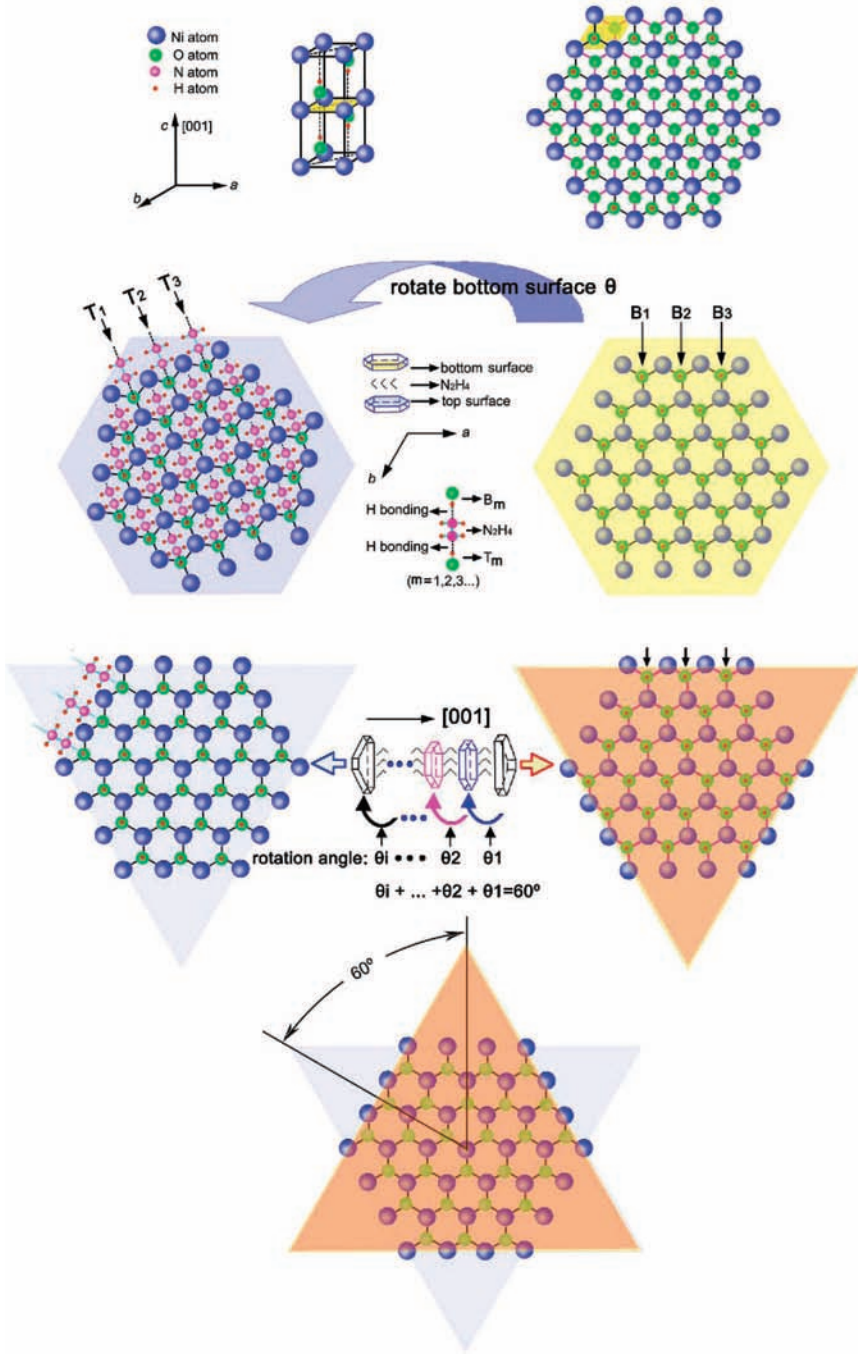

Figure 5. Illustration for the structure of the polyhedron with included angle of 60°. It shows the crystal structures of β-$Ni(OH)_2$ plates along the *c* axis and within the basal plane and tells how the N_2H_4 molecules link the $Ni(OH)_2$ plates through hydrogen bonding.

product were polished and smoothened, and the concave polyhedron was formed (in Figure 4c) in the end. From the top view and the developed view of the sides, it clearly reveals that the polyhedron has two regular triangles at the ends and six curved quasi-triangular surfaces on the side. The growth process could be proved by a broken intermediate polyhedron (in Figure S7 of Supporting Information), which shows the polyhedron structure is formed by multiple layers.

How does the elongated concave polyhedron achieve its intelligent growth with the 60° rotation between the two quasi-triangular-pyramids? Actually, the unique crystal structure of the nickel hydroxide could explain this interesting motif as illustrated in Figure 5.

The crystal structure of $Ni(OH)_2$ is shown in Figure 5 above viewing from different directions. The left one shows the structure along the *c* axis, i.e., the [001] direction. It exhibits the plane-asymmetry of hydroxyls on the yellow plane. The right one shows the corresponding structure within the yellow plane. It also shows two sets of hydroxyls on and within the yellow plane, revealing the crystal structures of the top and bottom surfaces of the precursor plates, respectively. The N_2H_4 molecules can link the plate precursor through the hydrogen bond resulting from a dipole−dipole force between an electronegative N atom of hydrazine and a hydrogen atom bonded to oxygen of nickel hydroxide, as shown in the middle of Figure 5.

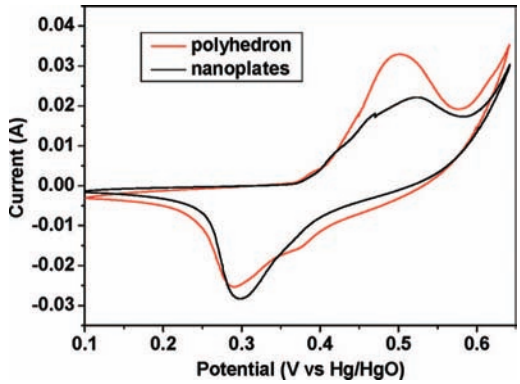

Figure 6. CV of Ni(OH)$_2$ polyhedrons and nanoplates at scan rate of 1 mV/s in 6 M KOH at room temperature.

To get two plates connected tightly with the N_2H_4 molecules, one plate need to take a rotation to better accommodate the H bonds and stabilize the structure. Because of the differences in the size and the shape of the plates (in Figure S1 of Supporting Information) as well as the asymmetry of the hydroxyl at the bottom and the top surfaces of the plates, each pair of plates would have a rotation angle to connect (the angles are marked with θ_1, θ_2,...). Figure 5 below shows the crystal structures (within the basal plane) of the top plate (the light red triangle) and the bottom plate (the light blue triangle) of one polyhedron. It is obvious that the angle would be 60° when one polyhedron forms through the linking plates layer by layer.

Because Ni(OH)$_2$ is used as positive electrode materials in Ni-based battery (Ni−MH, Ni−Fe, etc.), the good performance of Ni(OH)$_2$ is critical for battery. The morphology and size played an important role in determining the performance of Ni(OH)$_2$.[16,17] It has been reported that nickel hydroxide with a smaller crystalline sizes exhibited better charge−discharge cycling characteristics and a higher proton diffusion coefficient.[23] CV was used to evaluate the electrochemical performance of Ni(OH)$_2$ polyhedrons (samples in Figure 2) at a scan rate of 1 mV/s in 6 M KOH at room temperature. For comparison, Ni(OH)$_2$ nanoplate electrode (samples in Figure S1 of Supporting Information) was also constructed by the same procedure. Figure 6 shows the typical CV curves of polyhedron and nanoplates Ni(OH)$_2$ electrodes. In the range of scanning potentials employed, one anodic oxidation peak appearing at about 510 mV for polyhedron electrode. The oxidation peak is associated with the conversion of nickel hydroxide to nickel oxyhydroxide. Compared with the peak potential of polyhedron electrode, the oxidation peak for Ni(OH)$_2$ nanoplates shifted more positive potentials, indicating the oxidation process was favored for polyhedron electrode. The reduction peak appeared at about 291 and 297 mV for Ni(OH)$_2$ polyhedrons and nanoplates, respectively, which is associated with the conversion of oxyhydroxide back to nickel hydroxide.[24] The overall reaction is as follows

$$\mathrm{Ni(OH)_2 + OH^- \leftrightarrow NiO(OH) + H_2O + e}$$

The potential difference between anodic and cathodic peak positions (ΔE_p), is used to estimate of the reversibility of the electrode reaction. The ΔE_p value (0.210 V) of polyhedron electrode was smaller than that (0.227 V) of nanoplates electrode, which indicated the reversibility of redox reaction for the polyhedron electrode was better than nanoplate electrode. In all, the preliminary electrochemical experiment showed that polyhedron Ni(OH)$_2$ might have potential application in electrochemical storage.

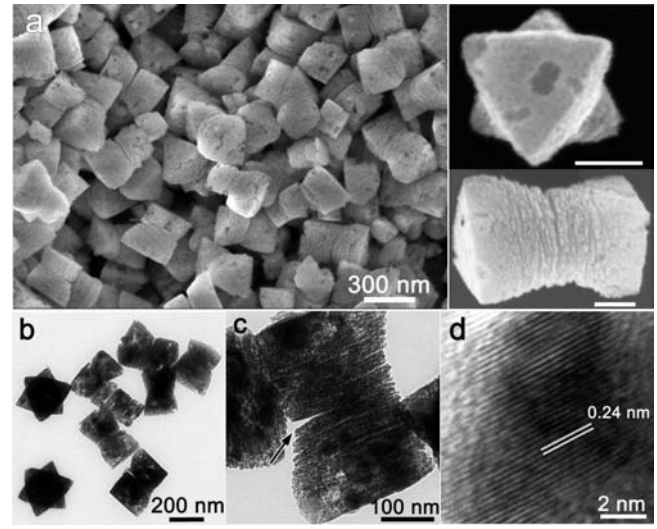

Figure 7. NiO prepared by heating β-Ni(OH)$_2$ at 500 °C for 1 h. (a) Overview of SEM image. Typical polyhedrons from the top and the side are shown on the right with both scale bars 100 nm. (b) TEM images of the sample. (c) A magnified image showing the lamellar structure. (d) HRTEM image corresponding to the region marked with an arrow.

It is well-known that nickel oxide with the unchangeable nanostructure can be obtained via a thermal decomposition of β-Ni(OH)$_2$ and some products became porous due to the dehydration.[10,18] We demonstrate here that single-crystal nickel oxide concave polyhedrons could be synthesized by calcinating the β-Ni(OH)$_2$ polyhedrons in nitrogen at 500 °C for 1 h (the XRD and SAED patterns are shown in Figure S8 of Supporting Information).

The size and morphology of the as-produced nickel oxide were examined with SEM and TEM in Figure 7. The overview of NiO in Figure 7a exhibits the same polyhedron structure with some pores on the surfaces. Typical top and side views of a polyhedron are shown on the side with both scale bars of 100 nm. The TEM image in Figure 7b further verifies the similar morphology of NiO. A magnified TEM image in Figure 7c clearly reveals that the polyhedron is accumulated by slice layers, which could be used to explain the textured character in the SAED pattern. The weaker link between two adjacent slices results in the partial split due to the dehydration process. HREM was performed on the thin edge marked with an arrow in Figure 7c. From Figure 7d, the interplanar distance is estimated to be 0.24 nm, corresponding to (111) plane of face-centered cubic NiO. All the characterizations demonstrate that the polyhedron nickel oxide has been fabricated by the dehydration of the as-grown Ni(OH)$_2$ polyhedrons.

Conclusion

To recapitulate, we have achieved a high-yield synthesis of single-crystalline nickel hydroxide polyhedrons by a facile wet chemical method. Here the nanobuilding blocks of nickel hydroxide nanoplates pile up together and grow along the [001] direction to form a novel geometry of concave polyhedron. The peculiar polyhedron crystals appear to arise

(23) Kalu, E. E.; Nwoga, T. T.; Srinivasan, V.; Weidner, J. W. *J. Power Sources* **2001**, *92*, 163–167.
(24) Watannabe, K.; Kikuoka, T. *J. Appl. Electrochem.* **1995**, *25*, 219–225.

from an intelligent growth and precise assembly oriented by the inherent spatial asymmetry of the nickel hydroxide crystal and directed by the hydrogen bonds with the added hydrazine molecules. The assembly is convergent in the sense that, by following the putative mechanism, a nearly identical morphology is obtained of elongated polyhedron with two precisely staggered triangular faces and tunable lengths up to 1 μm. Nickel oxide polyhedron crystals were also obtained with the preserved morphology by calcinations of the nickel hydroxide polyhedron crystals. Our work presented here not only adds a brand-new hierarchical structure but also illustrates the power of self-assembly in constructing some of the finest nanoarchitectures, which may be harnessed for building future nanodevices. The preliminary electrochemical experiments also show that $Ni(OH)_2$ polyhedrons might have potential application in electrochemical storage.

Acknowledgment. This project was financially supported by National Natural Science Foundation of China (50725208, 20673009, 20628303), State Key Project of Fundamental Research for Nanoscience and Nanotechnology (2006CB932301), National Basic Research Program of China (2007CB310500), Research Grant Council of Hong Kong (604206), and Specialized Research Fund for the Doctoral Program of Higher Education (20060006005) as well as by the Innovation Foundation of BUAA for PhD Graduates.

Supporting Information Available: Additional figures and experimental details. This material is available free of charge via the Internet at http://pubs.acs.org.

JA808784S